AMERICAN SOCIETY FOR MICROBIOLOGY | Journal of Bacteriology®

RESEARCH ARTICLE

From Intracellular Bacteria to Differentiated Bacteroids: Transcriptome and Metabolome Analysis in *Aeschynomene* Nodules Using the *Bradyrhizobium* sp. Strain ORS285 *bclA* Mutant

Florian Lamouche,[a] Anaïs Chaumeret,[a] Ibtissem Guefrachi,[a]* Quentin Barrière,[a] Olivier Pierre,[a]* Florence Guérard,[b] Françoise Gilard,[b] Eric Giraud,[c] Yves Dessaux,[a] Bertrand Gakière,[b] Tatiana Timchenko,[a] Attila Kereszt,[d] Peter Mergaert,[a] Benoit Alunni[a]

[a]Institute for Integrative Biology of the Cell, UMR 9198, CNRS/Université Paris-Sud/CEA, Gif-sur-Yvette, France

[b]Plateforme Métabolisme Métabolome, Institute of Plant Sciences Paris-Saclay, Centre National de la Recherche Scientifique, Institut National de la Recherche Agronomique, Université Paris-Sud, Université Evry, Université Paris-Diderot, Université Paris-Saclay, Orsay, France

[c]Laboratoire des Symbioses Tropicales et Méditerranéennes, Institut de Recherche pour le Développement, UMR IRD/SupAgro/INRA/UM2/CIRAD, Campus International de Baillarguet, Montpellier, France

[d]Biological Research Center, Hungarian Academy of Sciences, Szeged, Hungary

ABSTRACT Soil bacteria called rhizobia trigger the formation of root nodules on legume plants. The rhizobia infect these symbiotic organs and adopt an intracellular lifestyle within the nodule cells, where they differentiate into nitrogen-fixing bacteroids. Several legume lineages force their symbionts into an extreme cellular differentiation, comprising cell enlargement and genome endoreduplication. The antimicrobial peptide transporter BclA is a major determinant of this process in *Bradyrhizobium* sp. strain ORS285, a symbiont of *Aeschynomene* spp. In the absence of BclA, the bacteria proceed until the intracellular infection of nodule cells, but they cannot differentiate into enlarged polyploid and functional bacteroids. Thus, the *bclA* nodule bacteria constitute an intermediate stage between the free-living soil bacteria and the nitrogen-fixing bacteroids. Metabolomics on whole nodules of *Aeschynomene afraspera* and *Aeschynomene indica* infected with the wild type or the *bclA* mutant revealed 47 metabolites that differentially accumulated concomitantly with bacteroid differentiation. Bacterial transcriptome analysis of these nodules demonstrated that the intracellular settling of the rhizobia in the symbiotic nodule cells is accompanied by a first transcriptome switch involving several hundred upregulated and downregulated genes and a second switch accompanying the bacteroid differentiation, involving fewer genes but ones that are expressed to extremely elevated levels. The transcriptomes further suggested a dynamic role for oxygen and redox regulation of gene expression during nodule formation and a nonsymbiotic function of BclA. Together, our data uncover the metabolic and gene expression changes that accompany the transition from intracellular bacteria into differentiated nitrogen-fixing bacteroids.

IMPORTANCE Legume-rhizobium symbiosis is a major ecological process, fueling the biogeochemical nitrogen cycle with reduced nitrogen. It also represents a promising strategy to reduce the use of chemical nitrogen fertilizers in agriculture, thereby improving its sustainability. This interaction leads to the intracellular accommodation of rhizobia within plant cells of symbiotic organs, where they differentiate into nitrogen-fixing bacteroids. In specific legume clades, this differentiation process requires the bacterial transporter BclA to counteract antimicrobial peptides produced by the host. Transcriptome analysis of *Bradyrhizobium* wild-type and *bclA* mutant bacteria in culture and in symbiosis with *Aeschynomene* host plants dissected the

Citation Lamouche F, Chaumeret A, Guefrachi I, Barrière Q, Pierre O, Guérard F, Gilard F, Giraud E, Dessaux Y, Gakière B, Timchenko T, Kereszt A, Mergaert P, Alunni B. 2019. From intracellular bacteria to differentiated bacteroids: transcriptome and metabolome analysis in *Aeschynomene* nodules using the *Bradyrhizobium* sp. strain ORS285 *bclA* mutant. J Bacteriol 201:e00191-19. https://doi.org/10.1128/JB.00191-19.

Editor Anke Becker, Philipps-Universität Marburg

Address correspondence to Peter Mergaert, peter.mergaert@i2bc.paris-saclay.fr, or Benoit Alunni, benoit.alunni@i2bc.paris-saclay.fr.

* Present address: Ibtissem Guefrachi, Institut Sophia Agrobiotech, Sophia Antipolis, France; Olivier Pierre, Research Unit Biodiversity & Valorization of Arid Areas, Bioressources (BVBAA), Faculty of Sciences, Gabès University, Erriadh-Zrig, Gabès, Tunisia.

Received 12 March 2019
Accepted 31 May 2019
Accepted manuscript posted online 10 June 2019
Published 8 August 2019

bacterial transcriptional response in distinct phases and highlighted functions of the transporter in the free-living stage of the bacterial life cycle.

KEYWORDS BclA ABC transporter, legume-rhizobium symbiosis, metabolome, terminal bacteroid differentiation, transcriptome

Legume plants can fulfill their nitrogen requirements for growth under nitrogen-limiting conditions thanks to a symbiotic interaction with soil bacteria called rhizobia. The bacteria are housed in dedicated plant organs called nodules (1). Rhizobia are released within the symbiotic nodule cells by an endocytosis-like process and become nitrogen-fixing bacteroids. In several legume lineages, a terminal bacteroid differentiation (TBD) process occurs before effective nitrogen fixation is established. These bacteroids are enlarged and polyploid and have lost their capacity to produce offspring, hence the term TBD (2, 3). The host plant controls TBD by targeting defensin-like antimicrobial peptides called nodule-specific cysteine-rich (NCR) peptides to the bacteroids (4–6). This process requires the DNF1 protein, which is part of the signal peptidase complex that processes NCR peptides to allow their trafficking to the bacteroids by the secretory pathway (5, 7, 8). This particular type of symbiotic antimicrobial peptide has been found in two distinct legume families, the inverted-repeat-lacking clade (IRLC) (e.g., *Medicago* genus) and the Dalbergioids (e.g., *Aeschynomene* genus) (6, 9). However, the NCR peptides of those two families are not related and might have arisen by a convergent evolution process (6).

The successful completion of the TBD process also depends on bacterial factors, such as the BacA protein of *Sinorhizobium meliloti*, a symbiont of *Medicago* spp. (10). BacA is a transmembrane protein displaying similarities to the SbmA antimicrobial peptide transporter of *Escherichia coli*. These proteins are solely composed of an SbmA_BacA domain (pfam05992), which corresponds to a subfamily of transmembrane domains found in ABC transporters, although SbmA and BacA lack the ATPase domain usually present in this class of ATP-dependent transporters. The Δ*bacA* mutant of *S. meliloti* does not differentiate and undergoes rapid cell death after its release inside wild-type (WT) symbiotic plant cells (11). However, when the plant mutant *dnf1* is inoculated by the Δ*bacA* strain, bacteroids remain alive despite the fact that they fail to differentiate (11). Thus, BacA appears to be required to limit the antimicrobial activity of the NCRs. Furthermore, homologs of BacA in animal pathogens such as *Brucella abortus* and *Mycobacterium tuberculosis* are required to establish a chronic infection of the host, and they confer resistance to host defensins. The fact that these BacA proteins can fully or partially complement the Δ*bacA* mutant phenotype in *S. meliloti* suggests that this family of transporters is able to handle a broad range of antimicrobial peptides (12–15).

Bradyrhizobium sp. strains ORS278 and ORS285 possess a BacA-like transporter, named BclA, composed of a homologous SbmA_BacA transmembrane domain, as well as (and contrary to BacA or SbmA) a typical ATPase domain of ABC transporters. BclA is required for the establishment of a functional symbiosis with *Aeschynomene afraspera* and *Aeschynomene indica* (16, 17). Similar to the *S. meliloti bacA* mutant during nodulation of *Medicago*, the *Bradyrhizobium* Δ*bclA* mutants induce nodule formation in both *Aeschynomene* hosts and normally infect the nodule cells, but the intracellular bacteria fail to differentiate into polyploid and enlarged bacteroids. However, contrary to the *S. meliloti bacA* mutant, which dies rapidly after its release in *Medicago* species nodule cells and challenge with the NCR peptides, the undifferentiated Δ*bclA* nodule bacteria persist in the *Aeschynomene* nodule cells (17). The striking similarities in the TBD process between IRLC and Dalbergioid legumes, which is based on similar mechanisms from both the bacterial side (BacA-like transporters) and the plant side (NCR-like peptides), suggest a convergent coevolution in these distant legume clades and distant rhizobial species.

Bradyrhizobium sp. strain ORS285 can nodulate a large number of host species belonging to the *Aeschynomene* genus (6). In each of these hosts, the strain forms

bacteroids that have undergone the TBD process. However, the level of bacteroid differentiation and the type of bacteroids are different according to the host, and this correlates with the symbiotic efficiency of the symbiosis (6, 18). In some host species, such as *A. afraspera*, differentiation results in elongated bacteroids (E-type bacteroids) with moderate polyploidy, while in other species, e.g., *A. indica*, bacteroids are large spheres (S-type bacteroids) with high polyploidy. The latter are more efficient than the former (18, 19). In early nodule development on both host plants, bacteroids differentiate synchronously and very rapidly. Four days after nodule initiation, nodule cells are packed with undifferentiated bacteria, and 24 h later, bacteroids are formed and start fixing nitrogen while nodules continue to grow (20). In addition to the central nodule zone containing the bacteroid population, mature *A. afraspera* nodules have a peculiar outgrowth located on its tip that contains undifferentiated, saprophytic bacteria (20). This outgrowth is not formed in the nodules formed by the *bclA* mutant.

Transcriptome analysis of ORS285 in these two different *Aeschynomene* host plants with contrasting bacteroid types and efficiency has demonstrated that the transition from free-living bacteria to bacteroids is associated with a massive transcriptome switch involving about 20% of the protein-coding genes. Large gene sets are either up- or downregulated in one or both bacteroid types compared to levels in free-living bacteria (18). However, functional analysis of a selected subset of bacteroid-induced genes revealed no symbiotic defects in the mutants, suggesting the robustness of the bacterial symbiotic program or, alternatively, that some of the transcriptional responses are not related to the symbiotic nitrogen fixation process but simply reflect a response to the plant environment.

Because the symbiotic cells of nodules induced by the ORS285-Δ*bclA* mutant are fully infected but the bacteria are arrested before the TBD process and nitrogen fixation, the Δ*bclA* nodule bacteria can be seen as constituting an intermediate step in the formation of functional bacteroids. Previous macroarray- and microarray-based studies of the host and bacterial transcriptomes in the *S. meliloti bacA* mutant in interaction with *Medicago sativa* and *Medicago truncatula* were based on the same presumption (21–23). Thus, the Δ*bclA* mutant can be used as a tool to dissect this process and to study changes in nodule physiology and the response of bacteria in the plant environment before and after TBD and nitrogen fixation have taken place. In this study, we first analyzed the metabolome of *A. indica* and *A. afraspera* whole nodules elicited by the *Bradyrhizobium* sp. strain ORS285 wild type and Δ*bclA* mutant strains. We then compared the transcriptome profiles of the *Bradyrhizobium* sp. strain ORS285 wild type and the Δ*bclA* mutant in the exponential phase of culture and in nodules of *A. afraspera* and *A. indica*.

RESULTS AND DISCUSSION

Whole-nodule metabolomics shows a differential nitrogen metabolism between hosts and a reduced energy metabolism in mutant nodules. We determined in whole nodules, infected by the ORS285 wild-type strain or its Δ*bclA* mutant derivative, the relative levels of 129 metabolites and nucleotide cofactors by gas chromatography-mass spectrometry (GC-MS) and liquid chromatography-MS (LC-MS) analysis, respectively. Forty-seven metabolites accumulated differentially under the tested conditions (false discovery rate [FDR] of <0.05 and $P < 0.05$ by *post hoc* Tukey tests). These metabolites were grouped in four distinct classes. The first two classes comprise 27 and 7 metabolites differentially accumulated in wild-type-infected *A. indica* and *A. afraspera* nodules, respectively. Eight metabolites accumulated to higher levels in both wild type-infected nodules than in the corresponding nodules infected with the Δ*bclA* mutant, and six metabolites followed the opposite trend (see Fig. S1 and Table S1 in the supplemental material).

In legumes, there are two main forms of assimilated nitrogen that are exported from nodules to the aerial part of the plant. Depending on the plant species, these nitrogenous metabolites can be the amino acids asparagine (Asn) and glutamine (Gln), or they can be ureides, which are derived from purines (1). It seems that *A. indica* and *A. afraspera* have distinct strategies to transport fixed nitrogen to the other plant organs, with *A.*

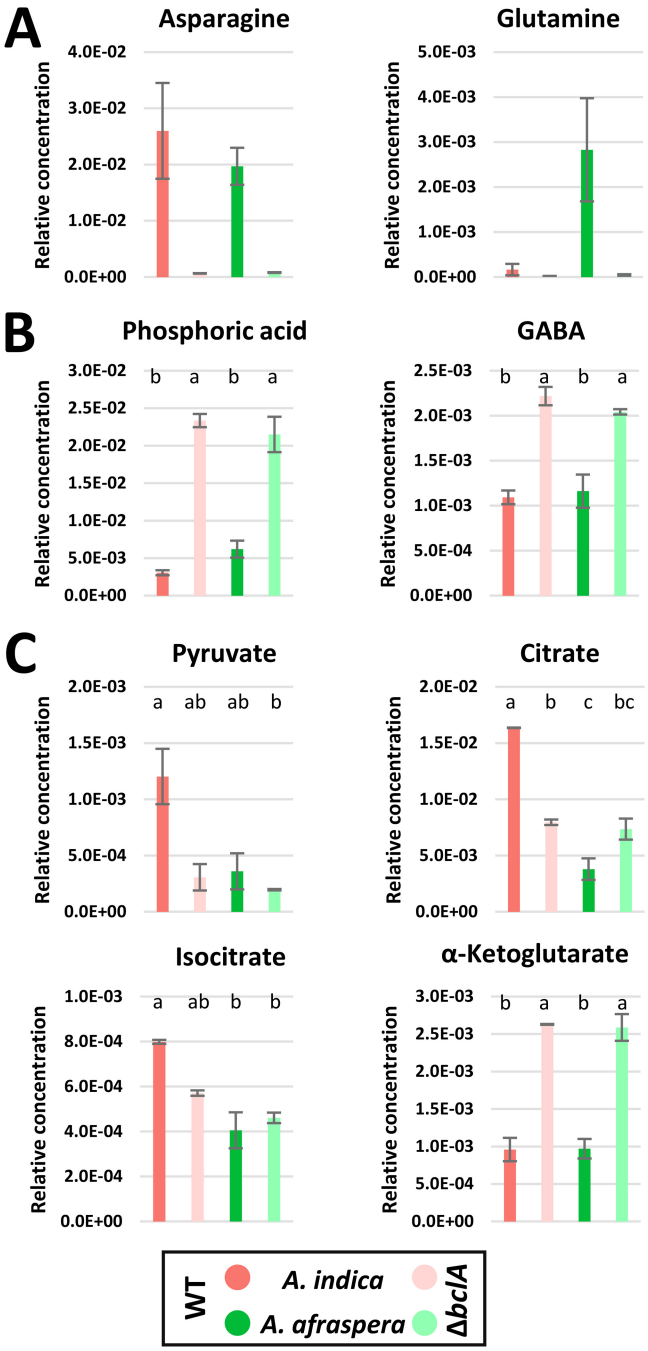

FIG 1 Whole-nodule metabolomics show significant differential accumulation of several metabolites in nodules elicited by Δ*bclA* bacteria. (A) *A. indica* and *A. afraspera* export distinct forms of nitrogen from nodules. (B) Nodules elicited by the Δ*bclA* strain accumulate phosphoric acid and γ-aminobutyric acid (GABA), suggesting limited phosphate uptake in bacteroids and plant nitrogen deficiency stress. (C) *A. indica* nodules display a higher primary metabolic rate leading to glutamate formation, suggesting a higher nitrogen fixation rate. Relative concentrations are expressed relative to internal standards. Data are means ($n = 2$) ± standard errors. Statistical significance was tested with one-way ANOVA (FDR of ≤0.05) and *post hoc* Tukey tests ($P < 0.05$), where different letters indicate significant differences.

afraspera exporting both Asn and Gln, whereas *A. indica* preferentially uses Asn as the exported form of nitrogen, as deduced from the accumulation of the corresponding metabolites in the symbiotic organs (Fig. 1A). These metabolites are not accumulated in the nonfixing nodules infected by the Δ*bclA* mutant bacteria.

Among the metabolites differentially accumulated in wild-type and Δ*bclA* nodules are phosphoric acid and γ-aminobutyric acid (GABA), which display higher concentra-

tions in the Δ*bclA* mutant-infected nodules than in the wild-type nodules (Fig. 1B). Phosphate is often seen as a limiting factor of nitrogen fixation (24). Indeed, the ORS285 strain shows a high expression of genes involved in phosphate and phosphonate import in wild-type bacteroids (18) as well as in the Δ*bclA* mutant nodule bacteria (see below). The accumulation of phosphoric acid could be due to an absence of its consumption by the nonfunctional Δ*bclA* nodules. The nodule bacteria require less phosphorus either because they require less ATP and energy or because they do not multiply their genome and, thus, store less phosphorus in their DNA. Alternatively, the host cells in these nonfunctional nodules consume less energy and ATP because no nitrogen is assimilated and transported, or a combination of the aforementioned processes contributes to the phosphoric acid accumulation. In the IRLC legume *M. truncatula*, GABA accumulates after a nitrogen deficiency stress and potentially induces nitrogen fixation (25). Accordingly, plants treated by GABA show increased nitrogen-fixing activity (26). Bearing this in mind, the GABA accumulation in *Aeschynomene* species nodules elicited by the Δ*bclA* strain could be a response of the plant to the deficient nitrogen fixation. Alternatively, as proposed for the *Pisum sativum-Rhizobium leguminosarum* association (27), GABA could be an amino acid source for the nodule bacteria provided by the plant. Its accumulation in nodules elicited by the Δ*bclA* strain could be due to the absence of its consumption by the nonfunctional nodule bacteria.

Further focusing on the Krebs cycle, *A. indica* nodules infected with the wild-type strain seem to have a higher level of the metabolites pyruvate, citrate, and isocitrate than those under the three other conditions. However, the subsequent compound in the cycle, α-ketoglutarate, is more abundant in the nodules of both host plants infected with the Δ*bclA* mutant. Additionally, succinate, fumarate, and malate, the three other compounds of the Krebs cycle that were examined, do not change significantly under the four conditions (Fig. 1C and Fig. S1). The Krebs cycle operates in both the bacteroids and the host cells, providing in both cell types reductant for ATP synthesis and, in the bacteroids, for nitrogen fixation. Moreover, the Krebs cycle also provides precursors in both cells for other pathways. In the bacteroids, α-ketoglutarate is the precursor for biosynthetic pathways such as amino acid synthesis (28, 29). In the host cell, the Krebs cycle furnishes the carbon source, mostly malate or succinate, that is transferred to the bacteroids, and α-ketoglutarate is the carbon skeleton for the assimilation of ammonium produced by the nitrogen-fixing bacteroids (1). Thus, the differential accumulation of the metabolites of the Krebs cycle in *A. indica* and *A. afraspera* nodules on the one hand and in nodules infected with the wild type or the Δ*bclA* mutant on the other hand possibly reflects differences in the nitrogen fixation rate between these nodules. Furthermore, the pools of ATP/ADP/AMP/NAD/NADP measured by LC-MS reflected high metabolic activities in wild-type bacteroids compared to those of the mutant, and we further observed slightly higher levels of those metabolites in *A. indica* bacteroids (Fig. S1). Together, these metabolic features support the previous observations of a higher symbiotic efficiency of S-type bacteroids in *A. indica* nodules than in *A. afraspera* E-type bacteroids (18, 19) and provide new insights on the possible underlying mechanisms (Fig. S2). The metabolome data further highlight a markedly different metabolism in the nodules infected with the Δ*bclA* mutant than wild-type nodules, and these differences were subsequently explored by a transcriptome analysis of the Δ*bclA* nodule bacteria.

General description of the transcriptome data set. We recently analyzed the transcriptome of wild-type *Bradyrhizobium* sp. strain ORS285 in symbiosis with *A. afraspera* and *A. indica* (18). Additional samples corresponding to the Δ*bclA* mutant were produced simultaneously, and the comparative analysis of these transcriptomes is presented here. Thus, the entire transcriptome data set (Table S2) is composed of the two bacterial genotypes (i.e., wild-type and Δ*bclA* genotypes), each in two host plants (i.e., *A. afraspera* and *A. indica* at 14 days postinfection [dpi]) and one culture condition, all produced and analyzed as biological triplicates (Fig. 2A). Principal component analysis revealed that Δ*bclA* bacteroids have a very different transcriptome from that of

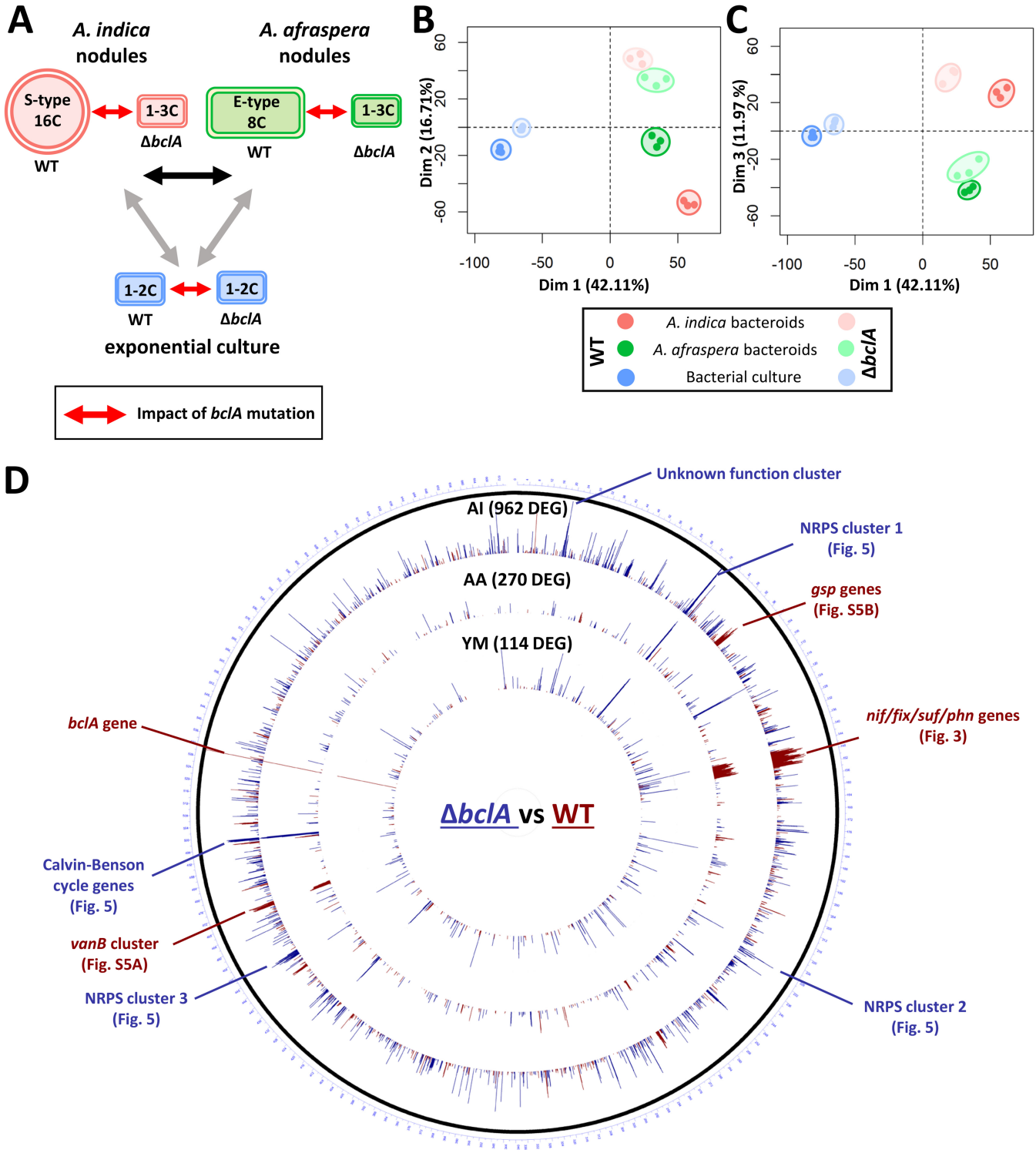

FIG 2 Experimental setup and general overview of the transcriptome data set. (A) Experimental setup displaying the six biological conditions and the comparisons of interest. Bacteroid-specific expression patterns (gray arrows) and host-specific genes (black arrow) of the wild-type (WT) bacterium were analyzed in reference 18. (B and C) Principal component analysis of the data set demonstrating the clear separation of the six conditions and the reproducibility of the biological replicates. (D) Circular representation of the *Bradyrhizobium* sp. strain ORS285 chromosome displaying the three comparisons between wild-type and Δ*bclA* strains. Blue and red peaks display upregulated and downregulated genes, respectively, in the Δ*bclA* strain compared to levels in the wild-type strain. Genes discussed in the text are indicated on the graph. AI, *Aeschynomene indica* bacteroids; AA, *Aeschynomene afraspera* bacteroids; YM, free-living culture; S-type, spherical bacteroids; E-type, elongated bacteroids.

the wild-type bacteroids. A clear partitioning of the samples was observed, with the first axis (42% of the observed variance) separating the culture from the nodule conditions, the second axis (17% of the observed variance) separating the Δ*bclA* nodule bacteria from wild-type bacteroids, and the third one (12% of the observed variance) separating the *A. indica* and *A. afraspera* hosts (Fig. 2B and C). The validity of the transcriptomic data set was independently assessed by quantitative reverse transcription-PCR (qRT-PCR) on a subset of 23 differentially regulated genes. The $\log_2$ fold changes (LFC) obtained by both techniques were compared and appeared to be consistent (linear regression [R^2] value of 0.75) (Fig. S3). A general comparison of the transcriptomes was obtained by a ratio of the read repartition between wild-type and Δ*bclA* conditions using the Cluster of Orthologous Genes (COG) classification (Fig. S4). This COG analysis for the wild-type strain only revealed that bacteroids display an upregulation of genes involved in energy production/conversion (COG class C) and inorganic ion transport/metabolism (COG class P) on the one hand and a drastic downregulation of genes involved in translation (COG class J), signal transduction (COG class T), secondary metabolite biosynthesis (COG class Q), and cell motility (COG class N) on the other hand (18). In striking contrast, the Δ*bclA* nodule bacteria displayed an opposite transcriptional response from that of the wild-type strain, with a downregulation of class C and P and an upregulation of all the other COG classes, highlighting the absence of the nitrogen-fixing metabolic specialization in the mutant nodule bacteria (Fig. S4). Among the most remarkable COG classes which were upregulated in Δ*bclA* nodule bacteria was COG class V (defense mechanisms) as well as COG class Q (secondary metabolite biosynthesis), which was upregulated under the three Δ*bclA* conditions. Additional precisions at the whole-genome level of differentially expressed gene regions were brought about by a circular representation of the three comparisons of interest on the physical map of the bacterial chromosome (Fig. 2D). The impact of the Δ*bclA* mutation on the bacterial transcriptome was highest in *A. indica*, with 962 differentially expressed genes (DEG; see Materials and Methods for chosen cutoffs) between the two bacterial genotypes, followed by *A. afraspera*, with symbiosis with 270 DEGs and only 114 DEGs between the two genotypes in free-living culture.

Mutation of the *bclA* gene has a very limited impact on bacterial gene expression in culture. Apart from the later-discussed expression of the nonribosomal peptide synthase 1 (NRPS 1), which is strongly enhanced in the mutant, the *bclA* deletion has a very limited effect on the transcriptome of free-living bacteria (Table S3). Among the other notable upregulated genes in the Δ*bclA* mutant cultures are several genes encoding putative multidrug resistance efflux pumps (genes BRAD285_v2_3072, BRAD285_v2_0212, and BRAD285_v2_1677 [genes 3072, 0212, and 1677; in the text and figures, gene designations are represented only by the final four-digit numerical value of their full BRAD285_v2_xxxx format]), potentially involved in the secretion of the product of the NRPS. The mutant bacteria also display an induction of genes encoding two isoquinoline 1 oxidoreductases (*iorA*_1 and *iorB* [genes 4928 and 4929]), possibly involved in the catabolism of xenobiotics. Additional interesting upregulated genes in the mutant are *lrgAB* (genes 0350 and 0351), encoding a stress-responsive putative regulator of murein hydrolase activity involved in peptidoglycan synthesis, the general stress response gene *csbD* (gene 5411), the envelope stress response gene *degP* (protease Do; gene 4589), and a gene encoding trehalose-phosphate synthase involved in the production of the osmoprotectant trehalose (genes 3396 and 3397). Remarkably, all of these stress-responsive genes (or a homologous trehalose-phosphate synthase gene) are also upregulated in wild-type nodules of *A. afraspera* and *A. indica* (18) as well as in nodules infected with the Δ*bclA* mutant (Table S3). This suggests that the absence of *bclA* directly or indirectly alters the regulation of these stress responses.

The transcriptome of Δ*bclA* nodule bacteria reveals a major transcriptome switch associated with intracellular infection before bacteroid formation. Our previous study on wild-type *Bradyrhizobium* sp. strain ORS285 showed 1,335 DEGs between bacteroid and culture conditions; 679 of them were upregulated in the bacteroids in both hosts, and 656 were downregulated in these bacteroids (18). The 679

genes upregulated in wild-type bacteroids were partitioned in seven gene categories based on their differential expression profiles in Δ*bclA* nodule bacteria and wild-type bacteroids (Fig. 3A and Table S4).

The first class (class I) contains only 10 genes which are upregulated in both Δ*bclA* nodule bacteria compared to levels in the wild-type bacteroids (Fig. 3B). Seven of these genes encode proteins of unknown function which are all predicted to be secretory proteins. In addition, the gene cluster 4913–4916 encodes proteins involved in glycogen metabolism and an ABC transporter. It is interesting that the *S. meliloti* ortholog of gene 4916 is upregulated when bacterial cultures are treated by NCR peptides (30). Thus, we can speculate that this gene is involved in the response to NCR peptides, which could be higher in the absence of BclA, since BclA provides protection against the activity of the NCR peptides (31).

The second class (class II) comprises 97 genes that are drastically upregulated in wild-type bacteroids compared to levels in bacteria in culture and that are not upregulated in the Δ*bclA* nodule bacteria (Fig. 3B and Fig. S5A). Among them is the genomic region containing the *nif*, *fix*, *suf*, and *mop* genes (i.e., 66 genes) that encode the core machinery for nitrogen fixation, including the NifHDK nitrogenase, and that represent by themselves more than 20% of the transcripts in wild-type bacteroids (18). Thus, this gene class potentially contains additional and novel genes with a role in the nitrogen fixation and/or bacteroid differentiation processes. The 5436–5451 cluster of genes, including a *vanB*-homologous gene, is part of this class (Fig. 3B and Fig. S5A). This gene set is specifically present in the photosynthetic bradyrhizobia symbionts of *Aeschynomene* spp. and absent from other bradyrhizobia and could be involved in the degradation of a plant-derived polymer, although the genes are poorly annotated and their specific biochemistry remains to be determined (18). Its expression pattern suggests a role of one or several genes in bacteroid differentiation or in the nitrogen fixation process even if a *vanB* insertion mutant does not display any symbiotic phenotype (18). Three additional small groups of genes are part of this class and therefore could be required for bacteroid differentiation or nitrogen fixation. The first one (gene cluster 0890–0891) encodes a DnaJ-like protein and a putative ferredoxin. The second one (gene cluster 3886–3889) also encodes a ferredoxin and three additional proteins of unknown function. The third one (gene cluster 5727–5730) contains four poorly annotated genes. These loci have not been functionally characterized yet, and it will be of interest to determine the symbiotic phenotype of mutants in these loci.

In contrast to class II, the other gene classes (classes III to VII; Fig. 3B) are composed of genes that are induced in the Δ*bclA* mutant nodule bacteria to levels similar to those in the wild-type bacteroids. Therefore, these genes are less likely to be involved in the bacteroid differentiation process and nitrogen fixation. The expression of these genes possibly is induced by the plant environment or the intracellular location of the bacteria. This is the case, for example, for the *phn* and *pstSCAB-phoUB* gene clusters encoding phosphate and phosphonate uptake and utilization functions. Similarly, the type II secretion system (*gsp*) cluster of strain ORS285 is activated in Δ*bclA* nodule bacteria, similar to the case for wild-type bacteroids (Fig. S5B). This suggests a role of this secretion system in plant colonization but not a requirement for bacteroid differentiation and nitrogen fixation; this is also in agreement with the absence of a symbiotic phenotype in *gsp* mutants (18). Also in this gene category are the *phyR-ecfG* regulatory genes involved in a general stress response in alphaproteobacteria. Mutants in these genes in *Bradyrhizobium diazoefficiens* USDA110 display a symbiotic phenotype in *Glycine max* nodules (32, 33). However, their expression pattern and mutant phenotypes suggest that these genes do not have a specific role in nitrogen fixation but rather are required for the early steps of colonization, infection, and nodule development (33). Thus, the induced expression of the ORS285 *phyR-ecfG* genes in the Δ*bclA* mutant nodule bacteria is congruent with the symbiotic function of the strain USDA110 genes. However, the expression of the genes disappears in USDA110 bacteroids of *G. max* nodules (33), while their expression remains high in the ORS285 bacteroids in the nodules of both *Aeschynomene* spp., indicating differences in the nature of the stress

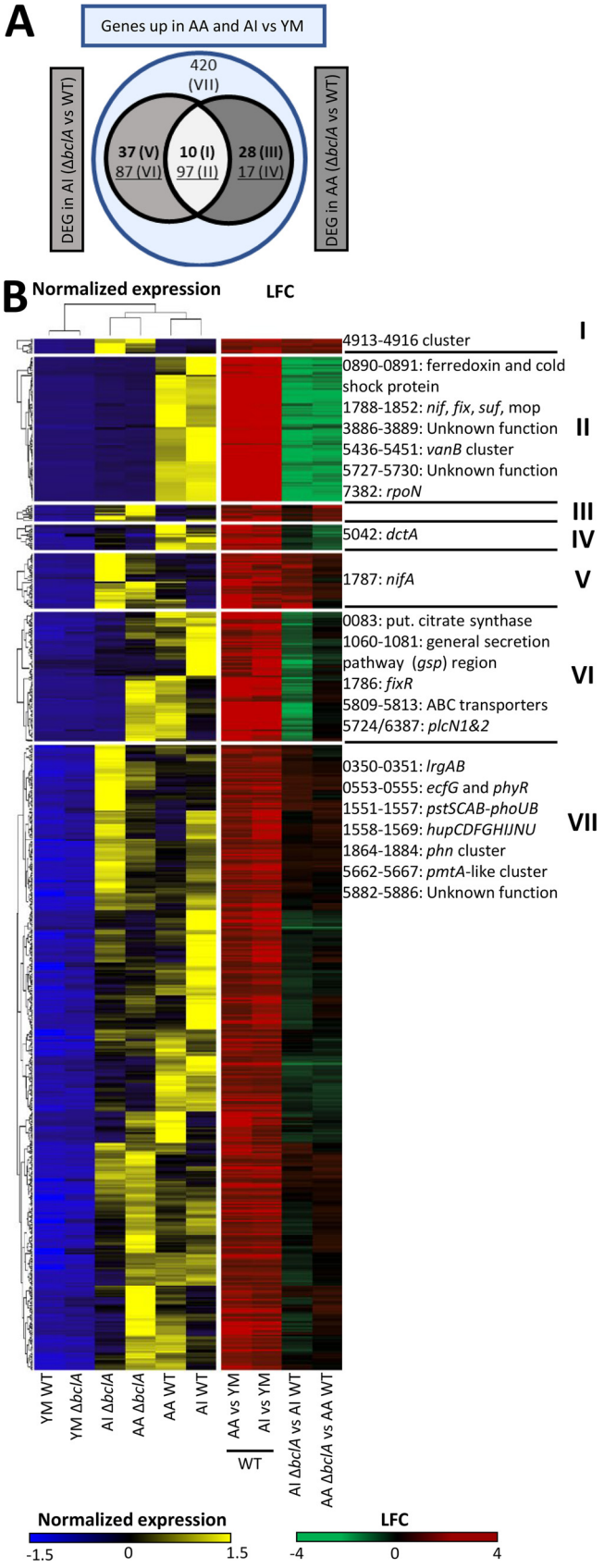

FIG 3 Expression of the bacteroid-specific genes in Δ*bclA* nodule bacteria. (A) Euler diagram showing the repartition of the 679 bacteroid upregulated genes (genes upregulated in *A. afraspera* nodules [AA] and

(Continued on next page)

condition or in its persistence in bacteroids in the USDA110-*G. max* and the ORS285-*Aeschynomene* species interactions.

Concerning the 656 downregulated genes in bacteroids (18), we found that the large majority of these genes are also downregulated in the Δ*bclA* mutant nodule bacteria (Fig. S6 and Table S5). Taken together, the expression of the large majority of the previously identified bacteroid-induced and -repressed genes is already modified in the nondifferentiated Δ*bclA* mutant nodule bacteria, indicating that a major transcription switch happens in the bradyrhizobia when they infect the nodule cells and before they differentiate. The subsequent differentiation into bacteroids and the nitrogen fixation process implicate a smaller number of genes, but those genes are activated to extremely high levels (18).

The transcriptome of Δ*bclA* nodule bacteria reveals a small number of host-specific and bacteroid-specific genes. We previously defined 515 host-specific genes that are differentially expressed between the two bacteroid types and that therefore potentially are involved in host-specific adaptations (18). As described above, gene expression in the Δ*bclA* nodule bacteria was used to discriminate among these genes between functions that are required for bacteroid differentiation in the specific host or genes whose expression is triggered by the intracellular infection in the specific host. Again, we find that the majority of genes with a host-specific expression pattern behave similarly in the Δ*bclA* nodule bacteria and in the wild-type bacteroids (Fig. S7 and Table S6). This confirms that the plant environment has a major impact on bacterial gene expression independent of the bacteroid differentiation and nitrogen fixation processes. Nevertheless, some gene clusters have an expression profile that is specific for functional bacteroids in a host-specific manner. Among the 515 host-specific genes, 268 genes have a higher expression in culture than under the *in planta* conditions. Another 112 genes were not differentially expressed in at least one comparison between the Δ*bclA* nodule bacteria and the corresponding wild-type bacteroid condition. Analysis of the remaining 135 genes partitioned these host-specific genes in a complex set of gene classes (k-means of 5) with specific expression patterns (Fig. 4 and Table S7).

One of these gene classes contains 54 genes specifically upregulated in *A. indica* bacteroids and not in the Δ*bclA* nodule bacteria (Fig. 4). This class contains a putative citrate synthase gene (gene 0083, one of the most highly expressed genes in *A. indica* bacteroids). The strong activity of this gene in the *A. indica* bacteroids could contribute to the differential accumulation of tricarboxylic acid cycle metabolites in the two bacteroid types and Δ*bclA* nodule bacteria (Fig. 1). This category further includes an ABC transporter (cluster 6210–6215), a very strongly expressed gene encoding a potential stress-related GTPase (gene 5408), and the 5532–5534 gene cluster of unknown function whose inactivation by mutation nevertheless did not provoke a symbiotic phenotype (18). Additional highly expressed gene sets that are part of this class are candidate genes for future functional analyses. They include the ModAB subunits of the molybdenum ABC transporter ModABC (gene cluster 5529–5530), two outer membrane protein complexes (genes 1686 and 1687 as well as 5529 and 5531), a stress-related gene encoding a CsbD-like protein (gene 5411), and the metabolic gene cluster 5128–5135.

FIG 3 Legend (Continued)
A. indica nodules [AI] versus the culture reference [YM], as defined in reference 18) according to their differential expression in Δ*bclA* nodule bacteria and in wild-type bacteroids (FDR of <0.01 and LFC of >1.58). Subgroups of differentially expressed genes in *A. indica* nodules (DEG in AI [Δ*bclA* mutant versus WT]) and *A. afraspera* nodules (DEG in AA [Δ*bclA* mutant versus WT]) or both are indicated. The majority (420) of bacteroid upregulated genes are not differentially expressed between the Δ*bclA* nodule bacteria and the wild-type bacteroids. Boldface and underlined numbers are upregulated and downregulated, respectively, under given conditions. The roman numerals between brackets refer to the clusters in panel B. (B) Heatmap and hierarchical clustering in seven classes of bacteroid-specific genes. Genes discussed in the text are indicated next to each class. The color-coded scale bars for the normalized expression and LFC of the genes are indicated below the heatmap. put., putative.

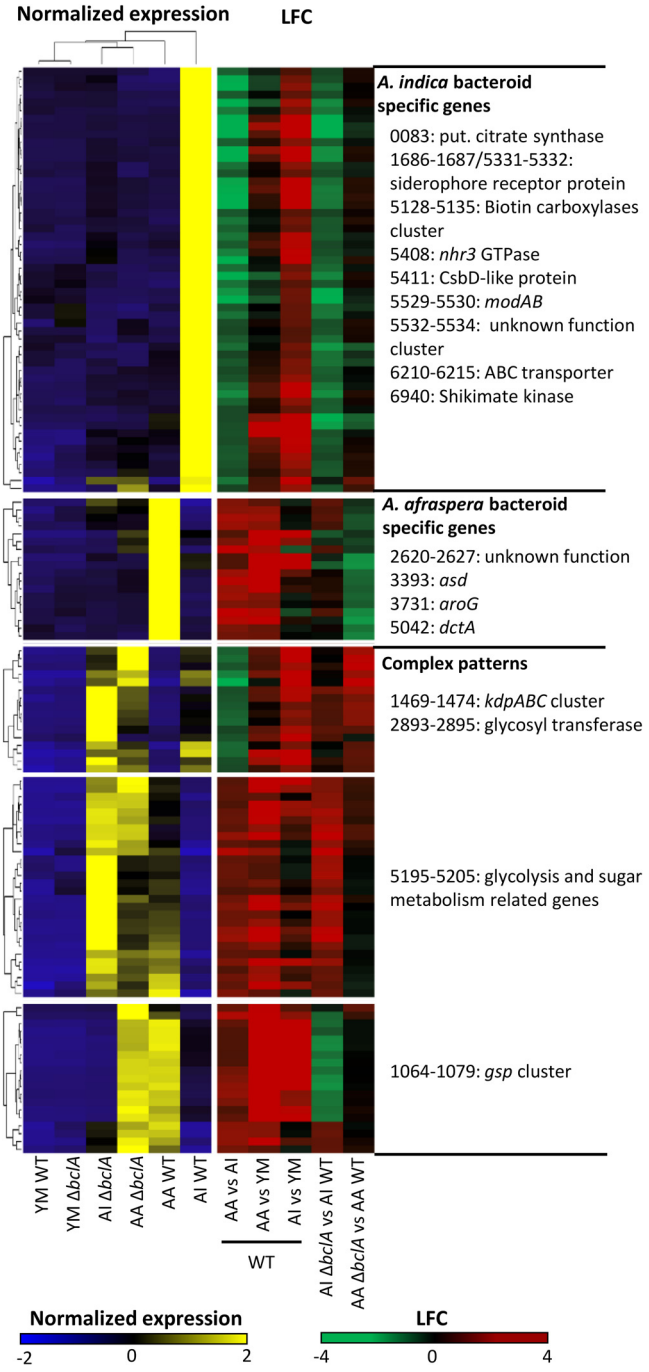

FIG 4 Expression pattern of 135 host- and bacteroid-specific genes with differential expression in Δ*bclA* nodule bacteria. Clusters were obtained by k-means clustering. Genes discussed in the text are indicated next to each class. The color-coded scale bars for the normalized expression and LFC of the genes are indicated below the heatmap.

A second class of 18 genes is composed of *A. afraspera*-specific genes that are not upregulated in the Δ*bclA* mutant in the *A. afraspera* nodule. This class contains *asd* (aspartate-semialdehyde dehydrogenase) and *aroG* (Shikimate kinase), which have no symbiotic phenotype when mutated (18). In addition, the gene class contains a putative cation efflux RND transporter (cluster 0387–0390), a poorly annotated gene cluster, 2620–2627, and the dicarboxylate transporter of gene *dctA*, already described in various studies as one of the main entry routes for plant carbon in the symbiotic bacterium (34).

Besides these two classes with a simple expression pattern, some additional classes have more complex expression profiles. Two of them contain genes that are activated in the Δ*bclA* nodule bacteria of both hosts and in the wild-type bacteroids of only one of the hosts (Fig. 4). The *kdpABC* locus (cluster 1469–1474) and the poorly annotated 2893–2895 cluster, probably involved in cellulose synthesis, are upregulated in the Δ*bclA* nodule bacteria and the *A. indica* wild-type bacteroids but not in the *A. afraspera* wild-type bacteroids. The *kdpABC* genes encode a potassium uptake transporter, and their role is most likely related to maintaining cell shape and turgor. Their expression patterns suggest that the stress factor inducing their expression is activated during the infection of the nodule cells in both hosts but is released in the *A. afraspera* bacteroids, while it is maintained in the *A. indica* nodules. Nevertheless, mutation of the *kdpA* and *kdpB* genes provokes no symbiotic defect on the two hosts (18). The other class of genes upregulated in the Δ*bclA* nodule bacteria and downregulated in *A. indica* bacteroids contains a large locus (5193–5209) potentially involved in the synthesis of a polysaccharide.

Another set of genes (0996, cluster 1025–1029, 1033, and cluster 2199–2206) with a complex expression pattern is highly expressed in culture (both in the wild type and the Δ*bclA* mutant), repressed in the Δ*bclA* nodule bacteria of both hosts, and activated in the *A. afraspera* wild-type nodule bacteria only (Fig. S7 and Table S6). These genes encode motility functions. Because motility has no meaning in bacteroids, which are immobile within the symbiosomes, this expression pattern could reflect the presence of saprophytic bacteria in *A. afraspera* wild-type nodules located in an outgrowth on the top of nodules (20).

The *bclA* mutation triggers the expression of nonribosomal peptide synthetases. *Bradyrhizobium* sp. strain ORS285 has the genetic repertoire for the production of several so-far-uncharacterized secondary metabolites, including one *N*-acyl homoserine lactone (AHL) and four peptides synthesized by NRPS gene clusters. Two of them display weak similarities to NRPS-producing ralsolamycin (used by *Ralstonia solanacearum* during colonization of fungal hyphae) and nostopeptolide (used by *Nostoc punctiforme* during symbiosis with plants) (18, 35, 36). The AHL gene cluster as well as three of the NRPS clusters are downregulated in bacteroids, while the NRPS 4 cluster is only weakly expressed, both in culture and in bacteroids (18). Strikingly, the expression in the free-living bacteria of the NRPS 1 gene cluster is strongly upregulated (more than 10-fold) in the Δ*bclA* mutant (Fig. 5A and Table S8). The NRPS 2 cluster, which is very strongly expressed in the wild type, is still expressed at a higher level in the mutant, albeit moderately (almost 2-fold), whereas the expression of two other NRPS and the AHL gene clusters is not significantly affected by the Δ*bclA* mutation. The upregulation of the NRPS 1 gene cluster in the free-living Δ*bclA* mutant is by far the most striking difference from the wild type (Fig. 5A and Table S8) and suggests a role of the BclA protein in the negative regulation of the NRPS 1 gene cluster and possibly also the NRPS 2 gene cluster. Discovering how exactly this nonsymbiotic function of BclA relates to the expression of NRPS genes will be a future challenge.

The AHL, NRPS 1, NRPS 2, and NRPS 3 gene clusters are also more strongly expressed in the Δ*bclA* mutant nodule bacteria than in the wild-type bacteroids (Fig. 5A and Table S8). Nevertheless, the expression of these genes in the Δ*bclA* mutant nodule bacteria is still severalfold lower than that in the free-living Δ*bclA* mutant (Fig. 5A and Table S8), suggesting that the downregulation of these gene clusters in bacteroids is, at least in part, independent of BclA. Moreover, the related *Bradyrhizobium* strain ORS278 lacks the NRPS gene clusters present in strain ORS285 and also has no additional ones (see Materials and Methods), but the ORS278 *bclA* mutant displays the same symbiotic defect as the ORS285 Δ*bclA* mutant (17). Together, these observations make it unlikely that the overexpression of the NRPS gene clusters and the potential production of toxic peptides in the Δ*bclA* mutant nodule bacteria is a major cause of the defective bacteroid differentiation in the mutant.

Gene expression in the Δ*bclA* nodule bacteria highlights the dynamics of interconnected oxygen and redox regulation during nodule development. Although regulation of nitrogenase gene expression has not been studied in *Bradyrhi-*

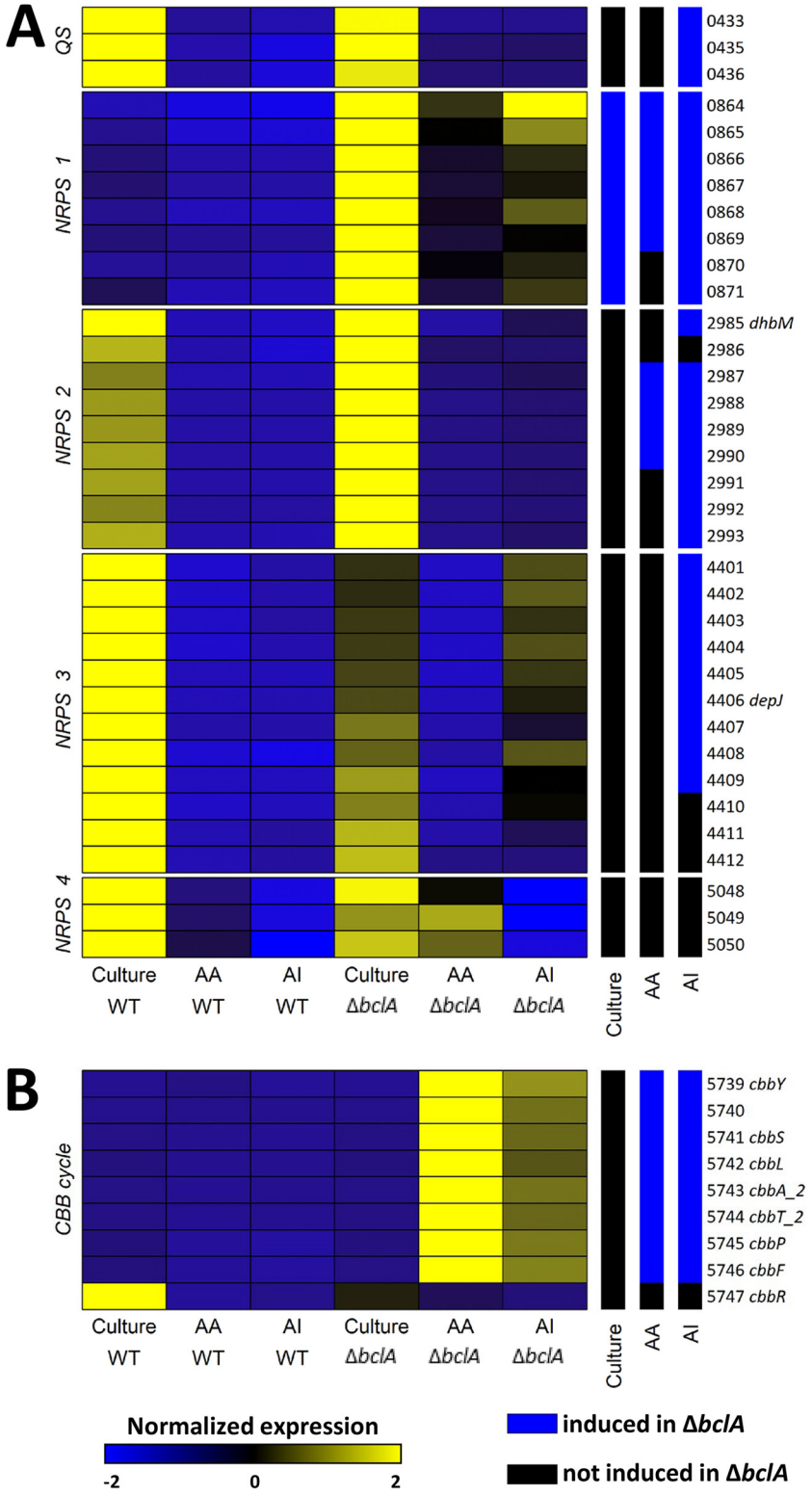

FIG 5 *bclA* mutation triggers the expression of nonribosomal peptide synthases (NRPS) and genes involved in the Calvin-Benson-Bassham cycle (CBB). (A and B) Heatmaps showing the gene expression of NRPS gene clusters (A) and CBB cycle genes (B) in *Bradyrhizobium* sp. strain ORS285 genome. NRPS genes are usually expressed under culture conditions and repressed in bacteroids, but the Δ*bclA* nodule bacteria display a higher expression of three NRPS clusters. The color-coded scale bar for the normalized expression is indicated. The CBB gene clusters are activated in the Δ*bclA* nodule bacteria. Right columns indicate whether the gene is induced in the Δ*bclA* strain (blue) or not (black) compared to induction in the wild type during free-living growth (culture) or in nodules of *A. afraspera* (AA) or *A. indica* (AI) (FDR of <0.01 and LFC of >1.58).

zobium sp. strain ORS285, it has been described in great detail in the related strain *B. diazoefficiens* USDA110 (28, 37), and the known regulators are conserved in ORS285. In strain USDA110, two interconnected oxygen-responsive regulatory cascades are present, the FixLJ-FixK2 and the RegSR-NifA-RpoN cascades of transcriptional regulators (38). The FixLJ-FixK2 cascade provides a gradual response to decreasing oxygen concentrations from 20% to 0.5%, while NifA is only active at low oxygen, below 2%. The two pathways are interconnected via RpoN. Expression of *rpoN* is regulated by the FixLJ-FixK2 pathway and encodes the alternative sigma factor σ^{54}, which activates the nitrogenase genes in concert with NifA. The expression of the *nifA* gene is regulated by the redox sensor RegSR, and the regulons of these regulatory modules have also been defined in USDA110 (39–45).

Based on the assumption that regulatory mechanisms are conserved between strains ORS285 and USDA110, we can interpret our transcriptome data set of the Δ*bclA* nodule bacteria. Neither *rpoN* (gene 7382) nor the nitrogenase genes were activated in the Δ*bclA* mutant nodule bacteria (the genes belong to the above-described class II shown in Fig. 3 and Table S4). On the other hand, the *nifA* gene (1787) was fully activated in the Δ*bclA* nodule bacteria (Table S4), suggesting that the signal sensed by RegS is present in these nodules. We also observe that the genes encoding the high-affinity *cbb3* terminal oxidase (the *ccoGHIS* and *ccoPQON* genes; cluster 4898–4905), required for bacteroid respiration and regulated by the FixLJ-FixK2 cascade in strain USDA110, were not fully activated in the Δ*bclA* mutant nodule bacteria (Table S2). On the other hand, the hydrogenase gene set (the *hup* gene cluster 1558–1569) and the nitrate reductase genes *napABCDE* (cluster 1014–1018), also regulated by FixK2 in response to low oxygen in strain USDA110 (51), were activated in the Δ*bclA* mutant nodule bacteria as in wild-type bacteroids (Table S2). In addition, the cytochrome *o* ubiquinol oxidase-encoding genes (*cyoABCD*; clusters 1590–1593 and 4945–4947), responsive to low oxygen and regulated by RegSR in strain USDA110 (44, 45), were slightly activated, especially in the *A. afraspera* nodules (Table S2). Together, the patterns of these nitrogen fixation genes in the Δ*bclA* mutant nodules suggest that oxygen levels are reduced relative to atmospheric levels but insufficiently to induce nitrogen fixation. This condition results in a partially activated FixLJ-FixK2 cascade and an inactive NifA. Moreover, the RegSR regulator seems to be fully activated in the Δ*bclA* mutant nodules, activating *nifA* expression.

The Calvin-Benson-Bassham (CBB) cycle genes (cluster 5739–5746) were strongly expressed in Δ*bclA* nodule bacteria and highly upregulated compared to those in the wild-type bacteroids and free-living bacteria, where they are expressed at only very low levels (Fig. 5B). This pattern suggests that the CBB cycle has a role in symbiosis, notably when the bacteria have infected the nodule cells but before the onset of nitrogen fixation. This proposition is in agreement with a previous study demonstrating that the CBB cycle in *Bradyrhizobium* sp. strain ORS278 is required for the establishment of a functional symbiosis with *A. indica*, where it could play a role in redox homeostasis as a transient electron sink during the transition to microoxia and before bacteroids are differentiated and fix nitrogen (46). Furthermore, it is worth mentioning that the use of the CBB cycle as a redox buffer has been documented in other, related bacteria belonging to the *Rhodospirillales*, *Rhodobacterales*, and *Rhizobiales*, where these genes are under the transcriptional control of RegSR (for reviews, see references 40 and 41). Thus, in the *Bradyrhizobium* sp. strain ORS285 Δ*bclA* nodule bacteria, the high activity of the CBB cycle might reflect this intermediate stage, after oxygen levels have dropped, as discussed above, but before nitrogen fixation. This also implies that the plant is not sanctioning the absence of effective nitrogen fixation by stopping carbon supply to the bacterium, although sanctions have been shown to be applicable to noncooperative rhizobia in other legume-rhizobium systems (47, 48).

Only a small set of genes are specifically differentially expressed in the Δ*bclA* nodule bacteria. The phenotype of the Δ*bclA* nodule bacteria is similar to that of the wild-type bacteria after their release and multiplication in the cells of the incipient nodule and before the onset of TBD and nitrogen fixation (17, 20). The above-described

gene expression patterns are in agreement with this proposition. However, we cannot exclude that the Δ*bclA* mutant also is engaged in a path that is not related to the wild-type symbiotic process. We reasoned that such a putative abnormal state of the Δ*bclA* nodule bacteria should be reflected in their transcriptome by the specific activation and/or repression of large sets of genes which are not regulated in the same way in the wild-type bacteroids. The search for genes with such an expression pattern in our data sets resulted in only a very small number of genes, 117 upregulated genes and 9 downregulated genes (Fig. S8 and Table S9). Among them are the above-described CBB cycle genes. Moreover, most of these genes are weakly or moderately expressed under all conditions. Thus, this analysis does not support the possibility of a strong change in the Δ*bclA* nodule bacteria that is not related to wild-type bacterial adaptation in nodule cells.

Conclusions. In this study, whole-nodule metabolomics combined with bacterial transcriptomics were used (i) to characterize at the molecular level the dysfunctioning of the *Bradyrhizobium* species Δ*bclA* mutant during free-living growth as well as in symbiosis with its hosts, *A. indica* and *A. afraspera*, and (ii) to identify key mechanisms of bacteroid differentiation and nitrogen fixation by comparing the wild-type bacteroid transcriptome to one of the Δ*bclA* mutant nodule bacteria, used as an intermediate step between the free-living and the TBD states of this bacterium.

The TBD condition of *Bradyrhizobium* sp. strain ORS285 in *Aeschynomene* nodules corresponds to a very specific physiological state characterized by a dramatically different transcriptome of these bacteroids compared to that of free-living bacteria, involving the strong up- or downregulation of a large proportion of the bacterial genome (18). We found that the transcriptome of the Δ*bclA* mutant nodule bacteria had both strong similarities to and differences with the transcriptome in wild-type bacteroids. Notably, we observed a very limited number of bacterial functions specifically induced or repressed in the Δ*bclA* nodule bacteria. This observation supports the idea that the transcriptome of the Δ*bclA* mutant is very close to what happens in the wild-type strain upon intracellular release, just before the onset of TBD and nitrogen fixation. Moreover, researchers should also be aware that the use of a developmentally blocked mutant can lead to a specific gene expression profile that does not reflect the temporary states of the nodulation program of the wild type. Nevertheless, and bearing these caveats and limitations in mind, the Δ*bclA* transcriptome enabled us to dissect the bacterial symbiotic transcriptome in two distinct, major waves. The first wave is activated in the Δ*bclA* nodule bacteria and involves the majority of genes of the symbiotic transcriptome; the second one is not activated in the Δ*bclA* nodule bacteria and implicates a smaller number of very strongly expressed genes in functional bacteroids. Our transcriptome analyses revealed that the oxygen level in the nodules could be an important factor that accompanies or even mediates the transition between the two waves. This observation is consistent with previous phenotypic analyses comparing wild-type and Δ*bclA* mutant strains in symbiosis with *A. afraspera* and *A. indica*, showing that the Δ*bclA* mutant nodule bacteria are arrested just before TBD, at a stage corresponding to an early infection step of the wild type (6, 17, 31). The unfinished symbiotic program in the bacteria is probably mirrored in the transcriptional program of the host, as revealed by the absence of production of oxygen-scavenging leghemoglobin in the Δ*bclA* mutant nodules (17). The latter explains why oxygen levels in nodules cannot drop sufficiently to allow the completion of the bacterial program. Thus, the NCR- and BclA-mediated TBD process is probably a checkpoint monitored by the host to complete its symbiotic program, as was proposed before for *M. truncatula* (23). Furthermore, the Δ*bclA* mutant transcriptome allowed us to identify candidate gene sets for further characterization that are activated in both hosts or in a single host only and that belong to the first wave, controlled by the plant or intracellular environment, or to the second wave, controlled by TBD. Overall, the function of the BclA protein marks a key phenotypic and transcriptome transition in the intracellular accommodation of *Bradyrhizobium* sp. strain ORS285 in *Aeschynomene* nodules (Fig. 6).

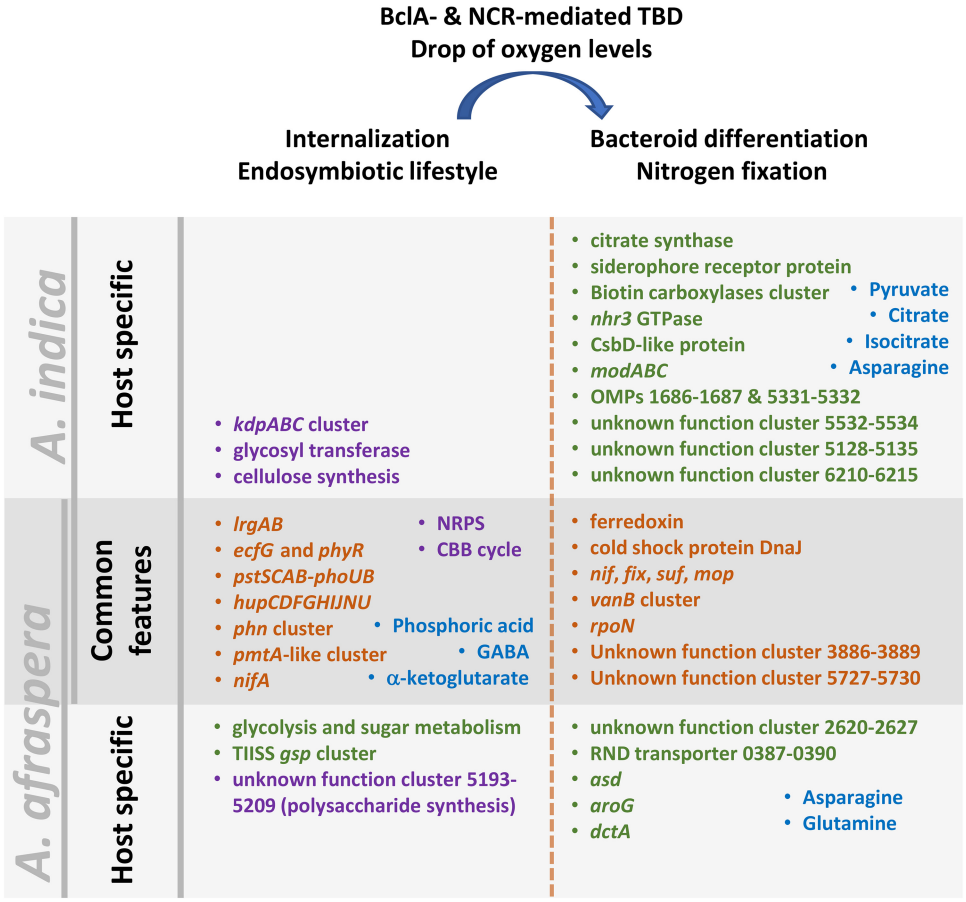

FIG 6 Metabolic and bacterial transcriptomic transitions during the intracellular bacterial infection and bacteroid differentiation in *Aeschynomene* species nodules infected with *Bradyrhizobium* sp. strain ORS285. Genes/functions in dark brown are commonly induced in both host species during the intracellular infection stage or bacteroid differentiation and nitrogen fixation. Genes/functions in green are activated in a host-specific manner, whereas purple ones are activated in the *bclA* mutant (intracellular infection stage) and repressed in mature wild-type bacteroids. Relevant metabolites detected by metabolomic analyses are in blue font.

Finally, we found that the Δ*bclA* mutation has a limited impact on the bacterial transcriptome under free-living conditions, although the higher expression of NRPS genes in the Δ*bclA* mutant suggests that the BclA function goes beyond the establishment of the nitrogen-fixing symbiosis. This peptide transporter may be involved in competition with other microbes mediated by NRPS-synthesized peptides. The wide conservation of this protein (17), including that in nonsymbiotic bacteria, is in agreement with a nonsymbiotic role of BclA during the free-living lifestyle of *Bradyrhizobium* sp. strain ORS285.

MATERIALS AND METHODS

Plant growth and inoculation. The *Bradyrhizobium* sp. strain ORS285 wild type and the Δ*bclA* mutant strain were grown at 30°C in YM medium supplemented with appropriate antibiotics (17). *A. indica* and *A. afraspera* plants were grown in transparent test tubes filled with BNM medium and inoculated with the desired strains as described before (18). Plants were grown at 28°C and 80% humidity in a 16 h/8 h light/dark regimen.

Metabolomic analyses. *A. afraspera* or *A. indica* nodules cultured for 14 dpi (pooled from more than 20 plants) and infected with the wild-type ORS285 or the Δ*bclA* mutant strain were collected in liquid nitrogen and lyophilized. Each sample was prepared in duplicate (biological replicates). Metabolites and cofactors were extracted from 100 mg or 800 mg of nodules and analyzed by GC-MS or LC-MS, respectively, according to reference 49. Relative concentrations of metabolites were determined relative to the internal standard ribitol, which was added after the grounding of the lyophilized material. Differential accumulation of metabolites was determined by one-way analysis of variance (ANOVA) (FDR of $\leq$0.05) and *post hoc* Tukey tests ($P < 0.05$). A heatmap of relative metabolite abundance (see Fig. S1 in the supplemental material) was produced using the ComplexHeatMap package (v 1.12) (50).

RNA extraction and transcriptomics. Nodules were harvested at 14 dpi. At this time point, nodules have grown to a large size that facilitates the harvesting of sufficient material for RNA extraction. Moreover, we have previously determined that at this age, the nodule cells are still fully infected with persistent Δ*bclA* bacteria and no signs of bacterial or plant cell degradation are observed (17). Nodule RNA was extracted from liquid nitrogen-frozen material according to reference 4. Nodule total RNA were depleted from plant/bacterial rRNA and eukaryotic mRNA using Ribo-Zero kits for plant seed/root and for Gram-negative bacteria (Epicentre, Madison, WI). Total RNA of bacterial cultures (grown in YM medium up to an optical density at 600 nm of 0.5) was extracted from liquid nitrogen-frozen pellets obtained using the hot phenol and hot SDS method (51). Oriented libraries of bacterial mRNA were produced and sequenced using the SOLiD technology (50-bp single read) as previously described (18). Here, we performed transcriptome sequencing (RNA-seq) analysis on the ORS285Δ*bclA* mutant strain in culture as well as in *A. afraspera* and *A. indica* nodules, resulting in the sequencing of 9 libraries (biological triplicates of each condition), which yielded ca. 30 million reads per sample, out of which ca. 9 million reads per sample were unique bacterial gene reads. The sequencing data of this project were submitted to the Sequence Read Archive (SRA) under accession no. GSE126971 (SRA number SRP186684). This data set of the Δ*bclA* mutant was generated simultaneously with the wild-type data set and compared with the previously published data set for the wild-type strain (GSE108744; SRA number SRP128034) (18).

qRT-PCR. Total RNA was extracted using the Plant RNeasy kit (Qiagen) and quantified before 2 μg RNA was DNase treated using the TurboDNA-free kit (Ambion, Life Technologies) and reverse transcribed with a RevertAid reverse transcriptase kit (Fermentas, Thermo Scientific). qRT-PCRs were performed using the LightCycler fast start DNA master SYBR green I kit on a Roche LightCycler 96 system (Roche) and the primers listed in reference 18. All kits were used according to the manufacturer's protocols. Cycling conditions were 95°C for 10 min, followed by 50 cycles at 95°C for 5 s, 58°C for 5 s, and 72°C for 15 s. The *rrs* 16S rRNA gene and the *miaB* gene (gene 7630) were used as references (18).

Statistical and differential expression analyses. Reads were trimmed, sized, and mapped on the reference genome of *Bradyrhizobium* sp. strain ORS285 (52) using CLC Workbench 10 software (CLC bio, Aarhus, Denmark). Unique gene reads mapping on ≥80% of their length and displaying ≥90% identity were considered for differential analyses. Only genes with a gene count over 1 count per million (cpm) in half of the samples of the data set were retained for further analysis. Normalization and differential analyses were performed using the DESeq2 package (version 1.12.4) (53). Wald tests from the DESeq2 package were used to compare gene expression values. The cutoff chosen for differentially expressed genes (DEG) are an FDR of <0.01 and a fold change of >3 ($\log_2$ fold change of >1.58). Principal component analysis of normalized data was computed using the FactoMineR package (v 1.33) (54). Heatmaps were produced using the ComplexHeatMap package (v 1.12) (50).

The ratio comparing read repartition between the two strains under the three conditions of the experimental setup, based on the COG database, was calculated as $R_i = \log_2[\sum$ reads Δ*bclA* $\text{COG}_i/(\sum$ reads WT $\text{COG}_i \times \text{sf})]$, with sf being the size factor depending on RNA-seq library size.

Genome mining analyses. The AntiSMASH software implemented on the MicroScope platform (55, 56) was used before to identify genes in the *Bradyrhizobium* sp. strain ORS285 genome possibly encoding enzymes involved in secondary metabolite synthesis (18). The same procedure was used here to analyze the *Bradyrhizobium* sp. strain ORS278 genome (57).

Data availability. The sequencing data of this project were submitted to the Sequence Read Archive (SRA) under accession no. GSE126971 (SRA number SRP186684).

SUPPLEMENTAL MATERIAL

Supplemental material for this article may be found at https://doi.org/10.1128/JB.00191-19.

SUPPLEMENTAL FILE 1, PDF file, 1.9 MB.

SUPPLEMENTAL FILE 2, XLSX file, 3 MB.

ACKNOWLEDGMENTS

F.L. and Q.B. were supported by Ph.D. fellowships from the Université Paris-Sud. The study was funded by the Agence Nationale de la Recherche, grant no. ANR-13-BSV7-0013. The work benefited from support by the Labex Saclay Plant Sciences (ANR-11-IDEX-0003-02) and used resources from the National Office for Research, Development, and Innovation of Hungary, grant no. 120120 to A.K.

REFERENCES

1. Udvardi M, Poole PS. 2013. Transport and metabolism in legume-rhizobia symbioses. Annu Rev Plant Biol 64:781–805. https://doi.org/10.1146/annurev-arplant-050312-120235.
2. Mergaert P, Uchiumi T, Alunni B, Evanno G, Cheron A, Catrice O, Mausset AE, Barloy-Hubler F, Galibert F, Kondorosi A, Kondorosi E. 2006. Eukaryotic control on bacterial cell cycle and differentiation in the rhizobium-legume symbiosis. Proc Natl Acad Sci U S A 103:5230–5235. https://doi.org/10.1073/pnas.0600912103.
3. Alunni B, Gourion B. 2016. Terminal bacteroid differentiation in the legume-rhizobium symbiosis: nodule-specific cysteine-rich peptides and beyond. New Phytol 211:411–417. https://doi.org/10.1111/nph.14025.
4. Mergaert P, Nikovics K, Kelemen Z, Maunoury N, Vaubert D, Kondorosi A, Kondorosi E. 2003. A novel family in *Medicago truncatula* consisting of more than 300 nodule-specific genes coding for small, secreted polypeptides with conserved cysteine motifs. Plant Physiol 132:161–173. https://doi.org/10.1104/pp.102.018192.

5. Van de Velde W, Zehirov G, Szatmari A, Debreczeny M, Ishihara H, Kevei Z, Farkas A, Mikulass K, Nagy A, Tiricz H, Satiat-Jeunemaître B, Alunni B, Bourge M, Kucho K, Abe M, Kereszt A, Maroti G, Uchiumi T, Kondorosi E, Mergaert P. 2010. Plant peptides govern terminal differentiation of bacteria in symbiosis. Science 327:1122–1126. https://doi.org/10.1126/science.1184057.
6. Czernic P, Gully D, Cartieaux F, Moulin L, Guefrachi I, Patrel D, Pierre O, Fardoux J, Chaintreuil C, Nguyen P, Gressent F, Da Silva C, Poulain J, Wincker P, Rofidal V, Hem S, Barrière Q, Arrighi JF, Mergaert P, Giraud E. 2015. Convergent evolution of endosymbiont differentiation in Dalbergioid and inverted repeat-lacking clade legumes mediated by nodule-specific cysteine-rich peptides. Plant Physiol 169:1254–1265. https://doi.org/10.1104/pp.15.00584.
7. Wang D, Griffitts J, Starker C, Fedorova E, Limpens E, Ivanov S, Bisseling T, Long S. 2010. A nodule-specific protein secretory pathway required for nitrogen-fixing symbiosis. Science 327:1126–1129. https://doi.org/10.1126/science.1184096.
8. Stonoha-Arther C, Wang D. 2018. Tough love: accommodating intracellular bacteria through directed secretion of antimicrobial peptides during the nitrogen-fixing symbiosis. Curr Opin Plant Biol 44:155–163. https://doi.org/10.1016/j.pbi.2018.04.017.
9. Montiel J, Downie JA, Farkas A, Bihari P, Herczeg R, Bálint B, Mergaert P, Kereszt A, Kondorosi E. 2017. Morphotype of bacteroids in different legumes correlates with the number and type of symbiotic NCR peptides. Proc Natl Acad Sci U S A 114:5041–5046. https://doi.org/10.1073/pnas.1704217114.
10. Glazebrook J, Ichige A, Walker GC. 1993. A *Rhizobium meliloti* homolog of the *Escherichia coli* peptide-antibiotic transport protein SbmA is essential for bacteroid development. Genes Dev 7:1485–1497. https://doi.org/10.1101/gad.7.8.1485.
11. Haag AF, Baloban M, Sani M, Kerscher B, Pierre O, Farkas A, Longhi R, Boncompagni E, Hérouart D, Dall'Angelo S, Kondorosi E, Zanda M, Mergaert P, Ferguson GP. 2011. Protection of *Sinorhizobium* against host cysteine-rich antimicrobial peptides is critical for symbiosis. PLoS Biol 9:e1001169. https://doi.org/10.1371/journal.pbio.1001169.
12. LeVier K, Phillips RW, Grippe VK, Roop RM, Walker GC. 2000. Similar requirements of a plant symbiont and a mammalian pathogen for prolonged intracellular survival. Science 287:2492–2493. https://doi.org/10.1126/science.287.5462.2492.
13. Domenech P, Kobayashi H, LeVier K, Walker GC, Barry CE. 2009. BacA, an ABC transporter involved in maintenance of chronic murine infections with *Mycobacterium tuberculosis*. J Bacteriol 191:477–485. https://doi.org/10.1128/JB.01132-08.
14. Wehmeier S, Arnold MFF, Marlow VL, Aouida M, Myka KK, Fletcher V, Benincasa M, Scocchi M, Ramotar D, Ferguson GP. 2010. Internalization of a thiazole-modified peptide in *Sinorhizobium meliloti* occurs by BacA-dependent and -independent mechanisms. Microbiology 156:2702–2713. https://doi.org/10.1099/mic.0.039909-0.
15. Arnold MFF, Haag AF, Capewell S, Boshoff HI, James EK, McDonald R, Mair I, Mitchell AM, Kerscher B, Mitchell TJ, Mergaert P, Barry CE, Scocchi M, Zanda M, Campopiano DJ, Ferguson GP. 2013. Partial complementation of *Sinorhizobium meliloti bacA* mutant phenotypes by the *Mycobacterium tuberculosis* BacA protein. J Bacteriol 195:389–398. https://doi.org/10.1128/JB.01445-12.
16. Bonaldi K, Gourion B, Fardoux J, Hannibal L, Cartieaux F, Boursot M, Vallenet D, Chaintreuil C, Prin Y, Nouwen N, Giraud E. 2010. Large-scale transposon mutagenesis of photosynthetic *Bradyrhizobium* sp. strain ORS278 reveals new genetic loci putatively important for Nod-independent symbiosis with *Aeschynomene indica*. Mol Plant Microbe Interact 23:760–770. https://doi.org/10.1094/MPMI-23-6-0760.
17. Guefrachi I, Pierre O, Timchenko T, Alunni B, Barrière Q, Czernic P, Villaécija-Aguilar JA, Verly C, Bourge M, Fardoux J, Mars M, Kondorosi E, Giraud E, Mergaert P. 2015. *Bradyrhizobium* BclA is a peptide transporter required for bacterial differentiation in symbiosis with *Aeschynomene* legumes. Mol Plant Microbe Interact 28:1155–1166. https://doi.org/10.1094/MPMI-04-15-0094-R.
18. Lamouche F, Gully D, Chaumeret A, Nouwen N, Verly C, Pierre O, Sciallano C, Fardoux J, Jeudy C, Szücs A, Mondy S, Salon C, Nagy I, Kereszt A, Dessaux Y, Giraud E, Mergaert P, Alunni B. 19 June 2018. Transcriptomic dissection of *Bradyrhizobium* sp. strain ORS285 in symbiosis with *Aeschynomene* spp. inducing different bacteroid morphotypes with contrasted symbiotic efficiency. Environ Microbiol. https://doi.org/10.1111/1462-2920.14292.
19. Lamouche F, Bonadé-Bottino N, Mergaert P, Alunni B. 2019. Symbiotic efficiency of spherical and elongated bacteroids in the *Aeschynomene-Bradyrhizobium* symbiosis. Front Plant Sci 10:377. https://doi.org/10.3389/fpls.2019.00377.
20. Bonaldi K, Gargani D, Prin Y, Fardoux J, Gully D, Nouwen N, Goormachtig S, Giraud E. 2011. Nodulation of *Aeschynomene afraspera* and *A. indica* by photosynthetic *Bradyrhizobium* sp. strain ORS285: the Nod-dependent versus the Nod-independent symbiotic interaction. Mol Plant Microbe Interact 24:1359–1371. https://doi.org/10.1094/MPMI-04-11-0093.
21. Ampe F, Kiss E, Sabourdy F, Batut J. 2003. Transcriptome analysis of *Sinorhizobium meliloti* during symbiosis. Genome Biol 4:R15. https://doi.org/10.1186/gb-2003-4-2-r15.
22. Capela D, Filipe C, Bobik C, Batut J, Bruand C. 2006. *Sinorhizobium meliloti* differentiation during symbiosis with alfalfa: a transcriptomic dissection. Mol Plant Microbe Interact 19:363–372. https://doi.org/10.1094/MPMI-19-0363.
23. Maunoury N, Redondo-Nieto M, Bourcy M, Van de Velde W, Alunni B, Laporte P, Durand P, Agier N, Marisa L, Vaubert D, Delacroix H, Duc G, Ratet P, Aggerbeck L, Kondorosi E, Mergaert P. 2010. Differentiation of symbiotic cells and endosymbionts in *Medicago truncatula* nodulation are coupled to two transcriptome-switches. PLoS One 5:e9519. https://doi.org/10.1371/journal.pone.0009519.
24. Sulieman S, Ha CV, Schulze J, Tran LSP. 2013. Growth and nodulation of symbiotic *Medicago truncatula* at different levels of phosphorus availability. J Exp Bot 64:2701–2712. https://doi.org/10.1093/jxb/ert122.
25. Sulieman S, Schulze J. 2010. Phloem-derived γ-aminobutyric acid (GABA) is involved in upregulating nodule N_2 fixation efficiency in the model legume *Medicago truncatula*. Plant Cell Environ 33:2162–2172. https://doi.org/10.1111/j.1365-3040.2010.02214.x.
26. Sulieman S. 2011. Does GABA increase the efficiency of symbiotic N_2 fixation in legumes? Plant Signal Behav 6:32–36. https://doi.org/10.4161/psb.6.1.14318.
27. Prell J, Bourdés A, Karunakaran R, Lopez-Gomez M, Poole P. 2009. Pathway of γ-aminobutyrate metabolism in *Rhizobium leguminosarum* 3841 and its role in symbiosis. J Bacteriol 191:2177–2186. https://doi.org/10.1128/JB.01714-08.
28. Terpolilli JJ, Hood GA, Poole PS. 2012. What determines the efficiency of N2-fixing *Rhizobium*-legume symbioses? Adv Microb Physiol 60:325–389. https://doi.org/10.1016/B978-0-12-398264-3.00005-X.
29. Terpolilli JJ, Masakapalli SK, Karunakaran R, Webb IUC, Green R, Watmough NJ, Kruger NJ, Ratcliffe RG, Poole PS. 2016. Lipogenesis and redox balance in nitrogen-fixing pea bacteroids. J Bacteriol 198:2864–2875. https://doi.org/10.1128/JB.00451-16.
30. Tiricz H, Szűcs A, Farkas A, Pap B, Lima RM, Maróti G, Kondorosi É, Kereszt A. 2013. Antimicrobial nodule-specific cysteine-rich peptides induce membrane depolarization-associated changes in the transcriptome of *Sinorhizobium meliloti*. Appl Environ Microbiol 79:6737–6746. https://doi.org/10.1128/AEM.01791-13.
31. Barrière Q, Guefrachi I, Gully D, Lamouche F, Pierre O, Fardoux J, Chaintreuil C, Alunni B, Timchenko T, Giraud E, Mergaert P. 2017. Integrated roles of BclA and DD-carboxypeptidase 1 in *Bradyrhizobium* differentiation within NCR-producing and NCR-lacking root nodules. Sci Rep 7:1–13. https://doi.org/10.1038/s41598-017-08830-0.
32. Gourion B, Sulser S, Frunzke J, Francez-Charlot A, Stiefel P, Pessi G, Vorholt JA, Fischer H-M. 2009. The PhyR-σEcfG signalling cascade is involved in stress response and symbiotic efficiency in *Bradyrhizobium japonicum*. Mol Microbiol 73:291–305. https://doi.org/10.1111/j.1365-2958.2009.06769.x.
33. Ledermann R, Bartsch I, Müller B, Wülser J, Fischer H-M. 2018. A functional general stress response of *Bradyrhizobium diazoefficiens* is required for early stages of host plant infection. Mol Plant Microbe Interact 31:537–547. https://doi.org/10.1094/MPMI-11-17-0284-R.
34. White J, Prell J, James EK, Poole P. 2007. Nutrient sharing between symbionts. Plant Physiol 144:604–614. https://doi.org/10.1104/pp.107.097741.
35. Spraker JE, Sanchez LM, Lowe TM, Dorrestein PC, Keller NP. 2016. *Ralstonia solanacearum* lipopeptide induces chlamydospore development in fungi and facilitates bacterial entry into fungal tissues. ISME J 10:2317–2330. https://doi.org/10.1038/ismej.2016.32.
36. Liaimer A, Helfrich EJN, Hinrichs K, Guljamow A, Ishida K, Hertweck C, Dittmann E. 2015. Nostopeptolide plays a governing role during cellular differentiation of the symbiotic cyanobacterium *Nostoc punctiforme*. Proc Natl Acad Sci U S A 112:1862–1867. https://doi.org/10.1073/pnas.1419543112.

37. Fischer H-M. 1994. Genetic regulation of nitrogen fixation in rhizobia. Microbiol Rev 58:352–386.
38. Sciotti MA, Chanfon A, Hennecke H, Fischer H-M. 2003. Disparate oxygen responsiveness of two regulatory cascades that control expression of symbiotic genes in *Bradyrhizobium japonicum*. J Bacteriol 185:5639–5642. https://doi.org/10.1128/JB.185.18.5639-5642.2003.
39. Lindemann A, Moser A, Pessi G, Hauser F, Friberg M, Hennecke H, Fischer H-M. 2007. New target genes controlled by the *Bradyrhizobium japonicum* two-component regulatory system RegSR. J Bacteriol 189:8928–8943. https://doi.org/10.1128/JB.01088-07.
40. Dubbs JM, Tabita FR. 2004. Regulators of nonsulfur purple phototrophic bacteria and the interactive control of CO_2 assimilation, nitrogen fixation, hydrogen metabolism and energy generation. FEMS Microbiol Rev 28:353–376. https://doi.org/10.1016/j.femsre.2004.01.002.
41. Elsen S, Swem LR, Swem DL, Bauer CE. 2004. RegB/RegA, a highly conserved redox-responding global two-component regulatory system. Microbiol Mol Biol Rev 68:263–279. https://doi.org/10.1128/MMBR.68.2.263-279.2004.
42. Durmowicz MC, Maier RJ. 1998. The FixK2 protein is involved in regulation of symbiotic hydrogenase expression in *Bradyrhizobium japonicum*. J Bacteriol 180:3253–3256.
43. Mesa S, Hauser F, Friberg M, Malaguti E, Fischer H-M, Hennecke H. 2008. Comprehensive assessment of the regulons controlled by the FixLJ-FixK2-FixK1 cascade in *Bradyrhizobium japonicum*. J Bacteriol 190:6568–6579. https://doi.org/10.1128/JB.00748-08.
44. Lunak ZR, Noel KD. 2015. A quinol oxidase, encoded by *cyoABCD*, is utilized to adapt to lower O_2 concentrations in *Rhizobium etli* CFN42. Microbiology 161:203–212. https://doi.org/10.1099/mic.0.083386-0.
45. Lunak ZR, Noel KD. 2015. Quinol oxidase encoded by *cyoABCD* in *Rhizobium etli* CFN42 is regulated by ActSR and is crucial for growth at low pH or low iron conditions. Microbiology 161:1806–1815. https://doi.org/10.1099/mic.0.000130.
46. Gourion B, Delmotte N, Bonaldi K, Nouwen N, Vorholt JA, Giraud E. 2011. Bacterial RuBisCO is required for efficient *Bradyrhizobium/Aeschynomene* symbiosis. PLoS One 6:1–9. https://doi.org/10.1371/journal.pone.0021900.
47. Kiers ET, Rousseau RA, West SA, Denison RF. 2003. Host sanctions and the legume–rhizobium mutualism. Nature 425:78–81. https://doi.org/10.1038/nature01931.
48. Westhoek A, Field E, Rehling F, Mulley G, Webb I, Poole PS, Turnbull LA. 2017. Policing the legume-Rhizobium symbiosis: a critical test of partner choice. Sci Rep 7:1419. https://doi.org/10.1038/s41598-017-01634-2.
49. Su F, Gilard F, Guérard F, Citerne S, Clément C, Vaillant-Gaveau N, Dhondt-Cordelier S. 2016. Spatio-temporal responses of *Arabidopsis* leaves in photosynthetic performance and metabolite contents to *Burkholderia phytofirmans* PsJN. Front Plant Sci 7:403. https://doi.org/10.3389/fpls.2016.00403.
50. Gu Z, Eils R, Schlesner M. 2016. Complex heatmaps reveal patterns and correlations in multidimensional genomic data. Bioinformatics 32:2847–2849. https://doi.org/10.1093/bioinformatics/btw313.
51. Chapelle E, Alunni B, Malfatti P, Solier L, Pédron J, Kraepiel Y, Van Gijsegem F. 2015. A straightforward and reliable method for bacterial *in planta* transcriptomics: application to the *Dickeya dadantii*/*Arabidopsis thaliana* pathosystem. Plant J 82:352–362. https://doi.org/10.1111/tpj.12812.
52. Gully D, Teulet A, Busset N, Nouwen N, Fardoux J, Rouy Z, Vallenet D, Cruveiller S, Giraud E. 2017. Complete genome sequence of Bradyrhizobium sp. ORS285, a photosynthetic strain able to establish Nod factor-dependent or Nod factor-independent symbiosis with *Aeschynomene legumes*. Genome Announc 5:e00421-17. https://doi.org/10.1128/genomeA.00421-17.
53. Love MI, Huber W, Anders S. 2014. Moderated estimation of fold change and dispersion for RNA-seq data with DESeq2. Genome Biol 15:1–21. https://doi.org/10.1186/s13059-014-0550-8.
54. Lê S, Josse J, Husson F. 2008. FactoMineR: an R package for multivariate analysis. J Stat Softw 25:1–18. https://doi.org/10.18637/jss.v025.i01.
55. Weber T, Blin K, Duddela S, Krug D, Kim HU, Bruccoleri R, Lee SY, Fischbach MA, Müller R, Wohlleben W, Breitling R, Takano E, Medema MH. 2015. AntiSMASH 3.0–a comprehensive resource for the genome mining of biosynthetic gene clusters. Nucleic Acids Res 43:W237–W243. https://doi.org/10.1093/nar/gkv437.
56. Vallenet D, Calteau A, Cruveiller S, Gachet M, Lajus A, Josso A, Mercier J, Renaux A, Rollin J, Rouy Z, Roche D, Scarpelli C, Médigue C. 2017. MicroScope in 2017: an expanding and evolving integrated resource for community expertise of microbial genomes. Nucleic Acids Res 45:D517–D528. https://doi.org/10.1093/nar/gkw1101.
57. Giraud E, Moulin L, Vallenet D, Barbe V, Cytryn E, Avarre J-C, Jaubert M, Simon D, Cartieaux F, Prin Y, Bena G, Hannibal L, Fardoux J, Kojadinovic M, Vuillet L, Lajus A, Cruveiller S, Rouy Z, Mangenot S, Segurens B, Dossat C, Franck WL, Chang WS, Saunders E, Bruce D, Richardson P, Normand P, Dreyfus B, Pignol D, Stacey G, Emerich D, Verméglio A, Médigue C, Sadowsky M. 2007. Legumes symbioses: absence of nod genes in photosynthetic bradyrhizobia. Science 316:1307–1312. https://doi.org/10.1126/science.1139548.